High-resolution neutron scattering measurement of the dynamic structure factor of heavy water

C. Petrillo* and F. Sacchetti
Istituto Nazionale per la Fisica della Materia, Unitá di Perugia, Perugia, Italy
and Dipartimento di Fisica, Università di Perugia, Via A. Pascoli, I-06123 Perugia, Italy

B. Dorner
Institut Laue Langevin, Boîte Postale 156, Grenoble, France

J.-B. Suck
Institute of Physics, Material Research and Liquids, TU Chemnitz, D-09107 Chemnitz, Germany
(Received 20 December 1999)

The low momentum collective dynamics of heavy water has been investigated by means of neutron three-axis spectroscopy. Working at the resolution limit of this instrument, an energy resolution of 2.6 meV was achieved for a constant analyzer energy of 120 meV. This good resolution allowed us to establish definitely that the collective dynamics of water is dominated by the presence and interaction of opticlike and acousticlike branches, coupling at wave-vector transfers of 0.3 to 0.35 $Å^{-1}$. The transition from slow to fast sound has been attributed to the interaction between opticlike modes and a solidlike fast acoustic mode.

PACS number(s): 61.12.Ex, 67.80.Cx, 62.60.+v

I. INTRODUCTION

Besides the special properties of water, which lead to an interest in its own, investigation of the dynamics of water has a general value because of the basic role which water plays in the existence and behavior of living systems. The dynamics of water has also attracted much attention because it is the prototype of a hydrogen-bonded network, where many of the complex features shown are connected to the presence of the medium strength hydrogen bonds. As the local structure of water is very close to that of its solid phase under normal conditions, i.e., hexagonal ice, it is quite reasonable to expect the dynamics of the liquid to be similar to that of the solid. In contrast to this anticipation, the sound velocity is in liquid water a factor of 2 smaller than in ice.

Recently, the dynamic structure factor of light water has been measured by ultrahigh resolution x-ray scattering [1–3] at low wave-vector transfer (from 0.2 to 1 $Å^{-1}$), in the meV energy range with a resolution of 1.5 meV. The results of this investigation add an important piece of information on the low momentum dynamics of water which was found to be more complex than expected from a previous neutron scattering study [4]. In particular, the fast sound, first observed by neutron scattering [4], was measured in more detail and the transition from the fast to the normal sound was investigated [2]. Moreover, the presence of an almost dispersionless mode was observed [3], thus introducing a further variable to the complex water dynamics. In Ref. [3] it was speculated that the dispersionless mode could have a connection with the low-lying optic mode of ice I_h [5], based on a comparison of the water spectra with those of ice measured under similar conditions, while the fast sound was related to a sort of solidlike behavior of the liquid at high frequency. The complexity of these features was taken as a possible explanation of the discrepancies existing between the results of the neutron scattering investigations reported in Refs. [4] and [6]. Indeed, no fast sound was reported in Ref. [6] although the absence of such a mode, which has a velocity of the order of 3000 m/s, could be due to the rather restricted dynamic range of this investigation. On the other hand, the almost dispersionless mode was observed in Ref. [6]. Finally, it must be mentioned that none of the available computer simulations give a full account of the experimental results, although some of the measured features are reproduced in old [7,8] and more recent computer simulations [9–11].

Considering that x-ray scattering experiments measure a dynamic structure factor which is related to the fluctuations of the electron density induced by the atomic motion and that the largest part of the electron density in water is concentrated on the oxygen site, it is evident that a neutron scattering investigation with adequate energy resolution and energy transfer range would be extremely desirable to obtain information also on the hydrogen dynamics. Of course, a neutron scattering measurement of the dynamic structure factor should be carried out on heavy water because of the huge incoherent cross section of hydrogen in light water. The favorable coupling of the neutron to the deuterium nucleus (coherent scattering) can be exploited to investigate the dynamics of deuterium, so that the comparison with the x-ray data, which mainly outline the oxygen motion, would enable a more detailed description of the collective dynamics of water. Moreover, a properly designed neutron scattering experiment, with a dynamic range wider than that achieved in the previous measurements [4,6], could help to solve the disagreements between the neutron results [4,6]. We therefore investigated the dynamic structure factor of heavy water by neutron inelastic scattering (NIS) in a wider energy range and with considerably improved resolution with respect to previous neutron scattering studies [4,6], using a configura-

*Present address: Dipartimento di Fisica, Politecnico di Milano, Piazza Leonardo da Vinci 32, 120133 Milano, Italy.

tion adequate to identify the fast sound as well as the new nondispersive mode observed in the x-ray scattering experiments. Finally, we believe that an additional experimental investigation of the nondispersive mode and its relation to the transition from the normal to the fast sound is necessary, since the presence of an opticlike mode in a liquid, the visibility of which should decrease with decreasing wave-vector transfer, is a rather surprising result worth a confirmation.

II. EXPERIMENT

The present measurements were carried out at the three-axis spectrometer IN1 installed at the hot source of the High Flux Reactor of the Institut Laue Langevin (Grenoble, France). The special properties of this instrument were fully exploited to succeed in this experiment. Due to the intense flux of high-energy neutrons provided by the hot source, the experiment could be performed with a rather high (constant analyzer) energy of 120 meV. Moreover, very tight collimations of 25′, 20′, 20′ and 20′ were employed from the reactor to the detector. This spectrometer configuration, in combination with the low background from an evacuated flight path around the sample, 1 m in diameter, allowed to collect high quality data down to 1° scattering angle. In order to improve the energy resolution, a vertically focusing Cu (331) monochromator and a vertically focusing Cu (400) analyzer were used. Pushing this spectrometer to its limits in resolution causes, however, a remarkable reduction in intensity.

A properly designed sample cell was employed to optimize this difficult experiment. The sample was contained in a flat, vacuum tight, $8\times4\times0.85\,\mathrm{cm}^3$ aluminum cell. The wall thickness was less than 1 mm but still thick enough to minimize the deformation of the cell under vacuum. In order to reduce the amount of multiple scattering, a honeycomblike Cd grid (0.6 cm edge) was mounted inside the cell. The effect of the Cd grid was to decompose the sample into many smaller samples having an almost cylindrical shape. This solution does practically not influence the transmission for the present experiment which is confined to the small wave-vector transfer region, where the scattering angle at the sample is always very small due to the rather high incoming energy. The Cd grid was found to reduce the multiple scattering contribution by more than a factor of 2.

All the measurements were carried out at 293 K on a 99.99% deuterated heavy water sample. The scattered intensity from the water sample was measured at five wave-vector transfers Q, namely at $Q=0.3$, 0.35, 0.4, 0.5, and 0.6 $\mathrm{Å}^{-1}$. Special attention was paid to the background subtraction, which, although rather small, is a non-negligible contribution especially to the tails of the scattering function. This is obvious taking into account that, at a given wave-vector transfer, the highest energy transfers are attained at the smallest scattering angles, i.e., next to the incident beam. The background from the empty cell, with the honeycomblike Cd grid in place, was measured at the same Q values as the sample, while the background produced outside the sample region was measured at $Q=0.3\,\mathrm{Å}^{-1}$ with the sample substituted by a highly absorbing 2 mm thick Cd plate. An additional measurement on the water sample after removing the Cd grid was carried out at $Q=0.3\,\mathrm{Å}^{-1}$. These data were used to check the multiple scattering correction. In order to measure

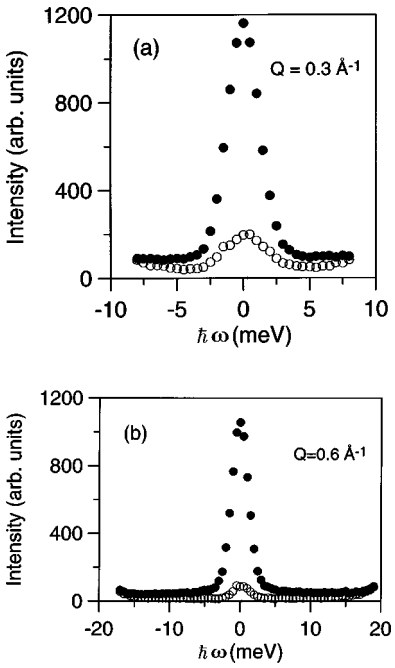

FIG. 1. Intensity versus energy transfer measured on the heavy water sample (dots) and the empty cell (circles). (a) Wave-vector transfer $Q=0.3\,\mathrm{Å}^{-1}$. (b) Wave-vector transfer $Q=0.6\,\mathrm{Å}^{-1}$.

the resolution of the instrument and for absolute normalization of the data, two scans at $Q=0.35\,\mathrm{Å}^{-1}$ and 0.5 $\mathrm{Å}^{-1}$ were performed by inserting a 2 mm tick Vanadium plate into the sample cell. As the Vanadium sample had the same extended size as the water sample, the normalization run was performed in exactly the same configuration as used for the sample measurements. Moreover, the same background was expected to affect the Vanadium measurements. This procedure minimizes the effect of the nonperfect uniformity of the incoming beam as both the sample and the Vanadium standard were uniform slabs with the same size.

After normalization of the measured data to the same monitor counts, the background intensity I_b to be subtracted from the data collected with the sample is given by the following standard relationship:

$$I_b=I_\alpha+T_b(I_e-I_a), \tag{1}$$

where I_e is the measured empty cell intensity, I_a is the intensity measured with the sample substituted by a full absorber (e.g., Cd) and T_b is the transmission of the sample for neutrons with 120 meV energy, i.e., the energy selected at the analyzer. In order to optimize the background subtraction and as the intensity from the absorber was measured only at $Q=0.3\,\mathrm{Å}^{-1}$, the contribution from the empty cell was analyzed at first. In Fig. 1 the intensity data measured from the sample at $Q=0.3\,\mathrm{Å}^{-1}$ and 0.6 $\mathrm{Å}^{-1}$ are shown in comparison with the corresponding empty cell data. From this figure it is apparent that the empty cell contribution, at the smallest scattering angles next to the incident beam, can be described by a rather smooth function reaching the higher values at the two ends of the scans and having a central peak, which seems to be due to an almost elastic process. In order to determine the best estimate for I_a, the empty cell data were plotted against the scattering angle 2ϑ. All the data, irrespec-

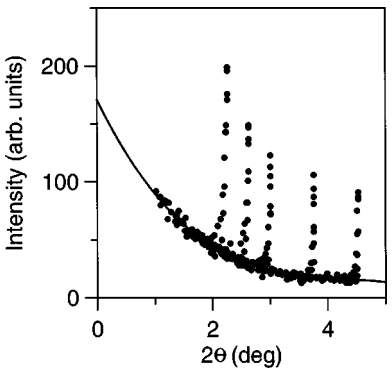

FIG. 2. Scattered intensity from the empty cell as measured in all the scans versus the scattering angle 2θ. The solid line is the best fit to the full data set excluding the elastic peaks.

tive of the energy transfer, are shown in Fig. 2. An inspection of this figure points out that the empty cell data lie on a single smooth curve which is independent of the energy transfer, apart from the elastic peak contributions which occur at different positions. It is therefore reasonable to assume the empty cell contribution be described by a smooth curve dependent only on the scattering angle plus an elastic peak which is probably due to small angle scattering of the aluminum container. This behavior is further emphasized in the measurement performed at 0.3 Å^{-1} with the sample substituted by the Cd plate. The resulting data are shown in Fig. 3 together with the empty cell data at the same wave-vector transfer. From Fig. 3 it is clearly seen that the elastic peak is due to the aluminum cell, as it is practically absent in the Cd data, whereas the remaining features of the spectrum are not affected by the addition of the Cd plate. Therefore, the intensity I_a was modeled by a smooth function of 2ϑ as obtained from a global fit to all the experimental data on the empty cell and the difference $(I_e - I_a)$ was obtained as the measured empty cell data minus this smooth function. The value of the transmission T_b for the D_2O sample, obtained using the measured heavy water cross section [12] at 120 meV neutron energy, turned out to be 0.70. By subtracting I_b from the intensity measured with the water sample in place, the scattering contribution due to the sample alone was deduced.

The background-free scattered intensity still contains the contribution from multiple scattering (MS) of the neutrons

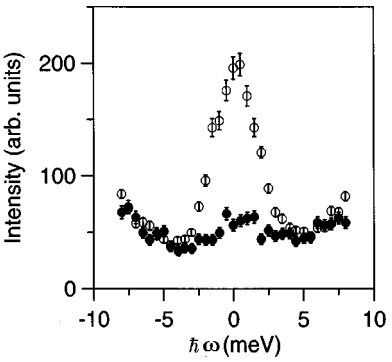

FIG. 3. Intensity versus energy transfer measured on the empty cell (circles) and the Cd absorber (dots) at the wave-vector transfer $Q = 0.3\ \text{Å}^{-1}$.

inside the D_2O cylinders. The evaluation of the MS is a complex task since the knowledge of the sample scattering function is required *a priori* at every incoming neutron energy. The scattering function of water, as obtained from medium resolution measurements and in a wide energy range, is reported in Ref. [13]. However, it appears quite difficult to include all the features of the experimental scattering function, which extends over an energy range in excess of 300 meV, in an MS simulation. Although the incoming energy never exceeded 140 meV in the present experiment, it seems almost impossible to have an accurate simulation of the MS on that fine mesh necessary to be used in the small energy range of the present measurements. Therefore, we preferred to model the scattering function of water by means of an analytic function as input for the MS simulation and to rely, at the same time, on the experimental data collected without the Cd grid, i.e., with an increased MS contribution, as a check of the accuracy of the simulation. The model scattering function had to be simple, however containing the most important features of the scattering function of water, relevant for an MS simulation. We assumed a scattering function consisting of a quasielastic contribution, accounting for the diffusionlike processes, plus a Gaussian peak which simulates the inelastic contributions. It was given by the following relationship:

$$S_{\text{mod}}(Q,\omega) = p_0 \frac{W}{\pi(\omega^2 + W^2)} + p_1 C_G e^{\beta\omega/2}\left[e^{-b(\omega-\omega_G)^2} + e^{-b(\omega+\omega_G)^2}\right], \tag{2}$$

where $p_0 = e^{-2W_D}$ is the measured Debye–Waller factor, $p_1 = 1 - p_0$ and $\beta = (1/k_B T)$. In the first term, describing the quasielastic scattering from the diffusing atoms, W is given by

$$W = \frac{\hbar D_0 Q^2}{1 + \tau D_0 Q^2},$$

where $D_0 = 2.2 \times 10^{-5}\ \text{cm}^2\,\text{s}^{-1}$ is the measured diffusion coefficient of water and $\tau = 0.5$ ps is the experimentally determined relaxation time [14]. In the Gaussian term, $b = 4 \ln 2 / W_G^2$ and W_G, ω_G, C_G are the full width at half maximum (FWHM), the center and the normalization factor of the Gaussian curve, respectively. W_G and ω_G were left as free parameters to be fixed by comparison with the experimental test data. The reasons for choosing such a model scattering function were supported by both the generally known water dynamics and the specific kinematic constraints of the present experiment. Indeed, because of the rather small energy range of the present measurements, most of the contributions to the MS were expected to come from the scattering function extending approximately over the same energy range. Moreover, considering the rather high incoming neutron energy, the high Q region of the scattering function was expected to mainly contribute to the MS. Therefore, the frequency dependence of the scattering function could be approximated by that appropriate for incoherent scattering, which probes diffusion processes and the density of states. It is important to observe that, since at high wave-vector transfers the quasielastic (diffusion) contribution is rather broad

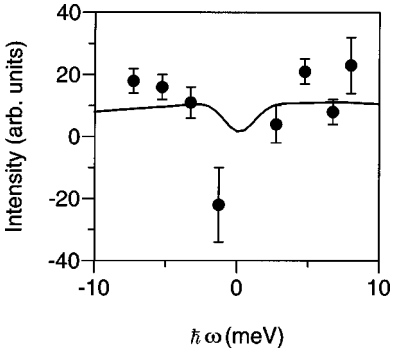

FIG. 4. Calculated multiple scattering contribution (solid line) in comparison with the experimental test data (dots) at $Q=0.3\,\text{Å}^{-1}$ and versus energy transfer. Both the experimental and the calculated data shown in the figure are obtained by taking the difference between the intensity scattered from the water sample without and with the Cd grid. The experimental data are binned to reduce the error.

and fairly small, genuine inelastic processes mainly contribute to the MS intensity which was then expected to be weakly dependent on energy. Moreover, no Q dependence of the MS contribution was expected considering that the present measurements were confined to the small Q region [15]. The MS simulation was carried out using a properly modified version of the simulation code which was successfully applied to the analysis of diffraction data [16]. Comparing the experimental data with the simulation results for the two cases with and without the Cd grid, we were able to fix the free parameters appearing in the scattering function. Quite generally, the simulation results confirmed the anticipations about the energy and wave-vector dependences of the MS contribution. It is worth noting that the results of the MS simulation were quite insensitive to the details of the scattering function, the most important parameter being the Debye–Waller factor which was fixed in agreement with the experimental data reported in Ref. [13]. The results of the MS simulation are shown in comparison with the experimental test data in Fig. 4, where it is observed that the simulation reproduces the experimental results rather well.

The calculated multiple scattering contribution was convoluted with the instrument resolution function, calculated according to the standard Cooper and Nathans [17] procedure using the known parameters of the instrument. The resulting intensity was then subtracted from the measured data. Using the measured vanadium data for normalization, the dynamic structure factor of the D_2O sample was obtained on an absolute scale. Finally, the incoherent contribution to the dynamic structure factor was subtracted by assuming it to be described by a very narrow Lorentzian function, as already introduced in Eq. (2). Since the width of this Lorentzian function was always smaller than $\sim$0.1 meV in the present Q range, the correction for the incoherent contribution amounted to the subtraction of a Gaussian function having the same width as the elastic resolution function. The resulting coherent dynamic structure factors are shown in Fig. 5 versus the energy transfer and at the different wave-vector transfer values.

The quality of the present data must be discussed in conjunction with the instrument resolution function. For this

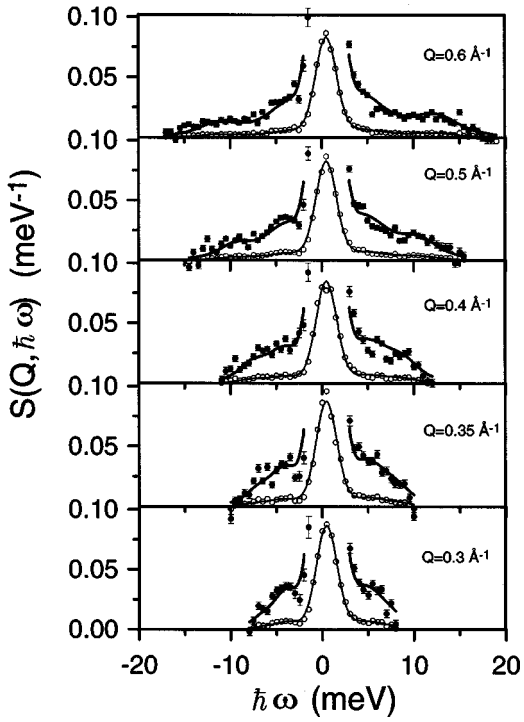

FIG. 5. Experimental dynamic structure factor of heavy water versus energy transfer and at the wave-vector transfer values of the measurements. The experimental data (circles) are also shown on a scale expanded by a factor of 5 (dots) to emphasize the inelastic structures. The solid lines are the curves calculated according to the fitted model described in the text.

purpose, the results obtained from the vanadium run, which is an experimental determination of the resolution, are shown in Fig. 6. The vanadium data were analyzed according to the same procedure as the water data. In Fig. 6 the energy resolution curve, expected with the present instrument configuration and calculated according to Ref. [17], is also shown. First of all, it is important to observe that the resolution is $\sim$2.6 meV FWHM, a value which is the top performance presently achievable on a three-axis at such a high incoming neutron energy. Moreover, such a resolution is comparable with the best ultrahigh resolution x-ray measurements which

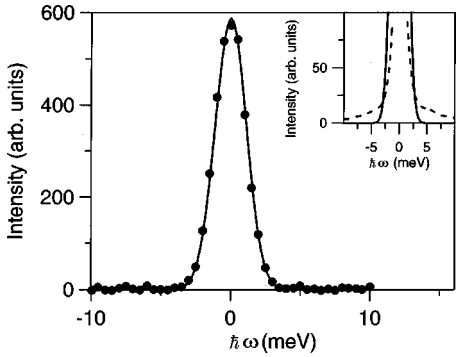

FIG. 6. Intensity versus energy transfer measured on the vanadium standard at $Q=0.5\,\text{Å}^{-1}$ (dots). The solid line is the calculated instrument resolution function. The inset shows the wings of the neutron and x-ray resolution functions on an expanded vertical scale. The solid line is the present resolution function and the dashed line is the resolution function of Ref. [3].

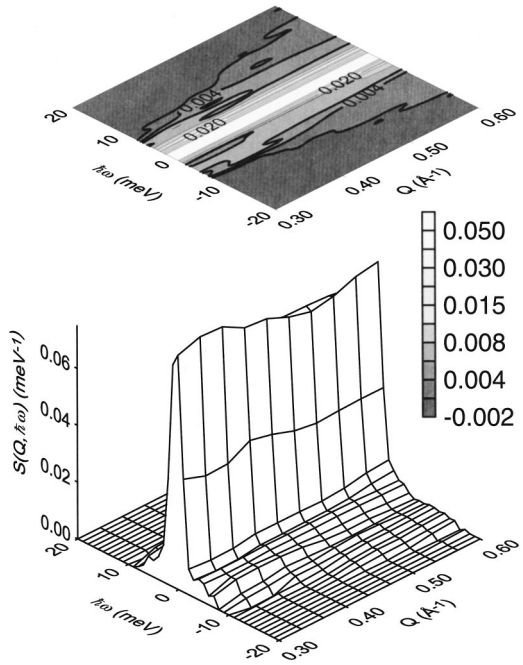

FIG. 7. Experimental scattering function in heavy water versus the energy transfer and the wave-vector transfer.

attain a FWHM of ~1.5 meV, although with the pronounced side wings arising from the almost Lorentzian resolution function characteristics of the x-ray spectrometers. On the contrary, the resolution function of a neutron three-axis spectrometer is practically a Gaussian (see inset in Fig. 6). The data in Fig. 6 also point out that the performances of the instrument were almost perfect as the agreement between the calculated resolution and the experimental data is excellent. Moreover, the wings of the measured resolution function are very symmetric as apparent from the extended and good-statistics scan shown in Fig. 6. Since the resolution function of the instrument is so symmetric and the wings of the vanadium scan do not extend into the inelastic part of the spectra, we are confident that the inelastic signal observed in all the scans on heavy water (Fig. 5) can safely be attributed to the sample response function.

A close inspection of Fig. 5 suggests a wave-vector-dependent structure of the inelastic signal, although it is rather complex. A guess on the general behavior of the dynamic structure factor can be obtained from the three-dimensional view of the data which is shown in Fig. 7. From this overall picture, both an almost wave-vector-independent mode and a dispersive mode can be identified. These results are in good qualitative agreement with the x-ray results. By inspection of the high Q region where $S(Q,\omega)$ departs from zero, one can infer a velocity of the dispersive mode in excess of 20 meV/Å^{-1}, that is larger than 3000 m/s. Such a value is much larger than the sound velocity in D_2O at 293 K measured by ultrasound spectroscopy [14], which is equal to 1360 m/s. This result, although obtained in a qualitative way, is in complete agreement with the results of Refs. [1] and [4].

III. DATA ANALYSIS AND DISCUSSION

More accurate results on the atomic dynamics in D_2O can be obtained by a quantitative analysis of the present data. In view of the complex behavior of the dynamic structure factor of D_2O, a data treatment based on a fitting of the experimental data to a damped harmonic oscillator model [1–4] seems a rather restrictive approach. The high number of parameters needed in such a fit would result in badly defined parameters leading to only qualitative conclusions as in the case of the analysis reported in Ref. [3]. Therefore, we tried to develop a model of empirical nature and requiring a smaller number of parameters to describe the basic physics in an intuitive fashion. The model exploits the observations reported in Refs. [1–4,6,18] in particular the presence of an almost dispersionless mode, which is evident in the density of states as measured in Ref. [18] by an incoherent neutron scattering experiment. The model should contain two modes with the following characteristics: one of the modes should be almost wave-vector-independent while the other has to be an acousticlike mode associated with a small velocity at low wave-vector transfer and a high velocity at high wave-vector transfer. A two-mode system having these characteristics is one where a wave-vector-independent mode interacts with an acoustic mode. If $\beta(Q)$ describes the interaction, the frequencies of the two modes, ω_+ and ω_-, are given by

$$\omega_+^2 = \tfrac{1}{2}[\omega_0^2 + \omega_a^2 + \sqrt{(\omega_0^2 - \omega_a^2)^2 + 4\beta^2}], \tag{3}$$

$$\omega_-^2 = \tfrac{1}{2}[\omega_0^2 + \omega_a^2 - \sqrt{(\omega_0^2 - \omega_a^2)^2 + 4\beta^2}], \tag{4}$$

where ω_0 is the frequency of the dispersionless mode and $\omega_a = c_\infty Q$ is the unperturbed acoustic dispersion relation, with c_∞ the sound velocity of the acoustic mode. If the interaction parameter $\beta(Q)$ depends linearly on Q, then the low Q sound velocity (normal sound) c_0 turns out to be given by

$$c_0 = \lim_{Q\to 0} \frac{\omega_-}{Q} = \sqrt{c_\infty^2 - \left(\frac{\beta}{Q\omega_0}\right)^2}. \tag{5}$$

At high Q the energy difference between the two modes increases and one expects the interaction to decrease with increasing Q value. Therefore a sensible choice for $\beta(Q)$ is the following:

$$\beta(Q) = \beta_0 Q \exp(-\lambda Q). \tag{6}$$

By means of Eq. (5), the model produces a sound velocity c_0 at low Q's which is smaller than c_∞ at high Q's. This finding resembles the results presented in Ref. [19] on the fast sound in a disparate-mass crystalline system and obtained from a well-founded calculation. As c_0 could have been determined only at lower Q values than accessible in the present experiment, we took $c_0 = 1360$ m/s from Ref. [14] and kept it fixed throughout the data analysis. In this way our model contains practically only two essential parameters c_∞ and ω_0, because β_0 is then defined by Eq. (5). The two-mode model was then described by the following coherent dynamic structure factor:

$$S_{\mathrm{coh}}(Q,\omega) = S_{\mathrm{el}}(Q,\omega) + S_-(Q,\omega) + S_+(Q,\omega), \tag{7}$$

where

$$S_{\mathrm{el}}(Q,\omega) = a_0(Q)\,\delta(\omega),$$

$$S_{\pm}(Q,\omega)=a_{\pm}(Q)\frac{1}{1-\exp(-\hbar\omega/k_BT)}\times\frac{\Gamma(Q,\omega)}{(\omega^2-\omega_{\pm}^2)^2+\Gamma^2(Q,\omega)},$$

that is the quasielastic peak was approximated by a δ function since, as also discussed previously, it is very narrow in the present experimental conditions. Moreover, each inelastic mode was assumed to be described by a damped harmonic oscillator with the same broadening function $\Gamma(Q,\omega)=\alpha Q\omega$ [15,20]. Equation (7) was fitted to the whole experimental data set leaving the coefficients $a_0(Q)$, $a_{\pm}(Q)$, α, c_{∞}, ω_0 and λ as free parameters. In this way the number of free parameters of the fit was reduced with respect to the procedure of Refs. [1–4] and the determination of the physically important parameters c_{∞} and ω_0 was more accurate. The fit was carried out by varying the four parameters α, c_{∞}, ω_0, and λ, which appear in the various equations in an entangled nonlinear form. The coefficients $a_0(Q)$ and $a_{\pm}(Q)$ were obtained for each choice of the four nonlinear parameters by a linear fitting to the data at each wave-vector transfer Q. The values of $a_{\pm}(Q)$ were finally used to derive integrated intensities $Z_{\pm}(Q)$, as we will discuss in the following. As our model depends explicitly on the wave-vector transfer Q, the model scattering function of Eq. (7) was convoluted with the four-dimensional $(\mathbf{Q},\omega)$-dependent resolution function.

The results of the fitting procedure are shown in Fig. 5 in comparison with the experimental data. Quite generally the quality of the fit is fairly good, as the model function reproduces the important features of the experimental scattering function. Therefore, we can consider the fitting parameters as meaningful within the present empirical model, especially the two parameters which define the dispersion relation, i.e., c_{∞} and ω_0. The best values obtained for c_{∞} and ω_0 were $c_{\infty}=21\pm2$ meV/Å^{-1}, that is 3200 ± 320 m/s, and $\hbar\omega_0=5.5\pm0.3$ meV. β_0, λ, and α turned out to be 105 ± 14 meV^2 Å, 3 ± 1 Å, and 10 ± 3 meV Å, respectively. The present value of $\hbar\omega_0$ is in very good agreement with the position of a clear peak in the density of states as measured in Ref. [18]. The value of c_{∞} is coincident with that deduced from the x-ray scattering data in light water [1–3] and very close to that obtained in a previous neutron experiment [4] carried out with a smaller incoming neutron energy and a broader resolution. The present results suggest that a confined dynamic range can cause a lack of observation of the fast sound, as it occurred in Ref. [6]. Indeed, the main difference between the present experiment and that of Ref. [6] is the minimum scattering angle achieved. A rather low scattering angle was instead obtained in the experiment reported in Ref. [4] and carried out on the IN8 spectrometer at the ILL. In that case, the dynamic range was wide enough to detect the fast sound. On the other hand, the experiment of Ref. [6] was carried out on the time-of-flight spectrometer MARI at the neutron spallation source ISIS and the minimum scattering angle was slightly larger. In fact, the experiment on MARI stimulated a more detailed search for signals from the ω_0 mode. Finally, the present data on the sound propagation in water show that the isotopic effect on the propagation of the fast sound is negligible, as it is the case for the normal sound velocity. This result, which was already suggested in Ref. [1], is apparent from the comparison between the present data in D_2O and the data of Refs. [1–3] in H_2O.

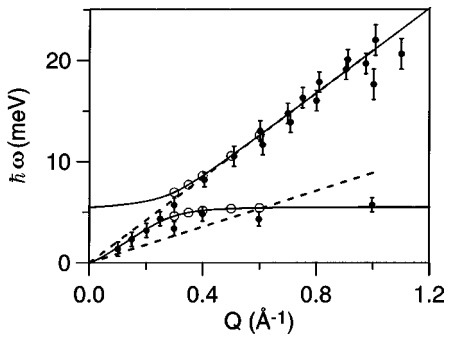

FIG. 8. Dispersion relation as deduced from the present experiment (solid line) in comparison with the results of the x-ray scattering experiments reported in Refs. [1–3] (dots). The open symbols indicate the results from neutron scattering. They lie necessarily on the calculated curves (see text). The dashed lines are reference linear dispersion curves corresponding to the velocities c_{∞} and c_0 (see text).

A more quantitative comparison with the x-ray experiment is obtained by superimposing the x-ray data to the dispersion relation produced by using the best-fit parameters of the present experiment. The plot is shown in Fig. 8 where, for clarity, we indicate by open circles the frequencies as obtained from the neutron experiment. This presentation is redundant because the circles lie necessarily on the dispersion curves as obtained by the fits. Nevertheless, the circles indicate from which data the dispersion curves were derived. The agreement observed in Fig. 8 shows that the interpretation of the data by the described model is meaningful as different approaches were followed to reduce the x-ray data. It is very interesting to observe that the lower branch of the present model fits extremely well the data obtained by x-ray scattering, and this is a region where both experiments are at their technical limits. The present model was also applied to fit the x-ray data by holding fixed the parameters α, c_{∞}, ω_0, and λ and leaving the coefficients $a_0(Q)$ and $a_{\pm}(Q)$ as free parameters. The fit performed at $Q=0.4$ Å^{-1} is shown in Fig. 9 where, again, a very good agreement between the model and the experimental results was found.

Finally the mode strengths as measured by the integrals

$$Z_{\pm}(Q)=\frac{1}{2}\int_{-\infty}^{+\infty}d\omega\,S_{\pm}(Q,\omega)$$

of the two modes comprised in the present model were calculated. In the classical limit [20], under the assumption of a solidlike behavior of the system, the integral is given by

$$Z_{\pm}(Q)=\frac{(\hbar Q)^2}{2M}\frac{k_BT}{(\hbar\omega_{\pm})^2}F_{\pm}^2(Q), \tag{8}$$

where $F_{\pm}(Q)$ are the structure factors of the modes and M is the mass of the molecule. Note that $Z_{\pm}(Q)$ does not depend on the damping Γ. The experimental values of $Z_{\pm}(Q)$ are given in Table I. In Fig. 10 we plot the structure factors

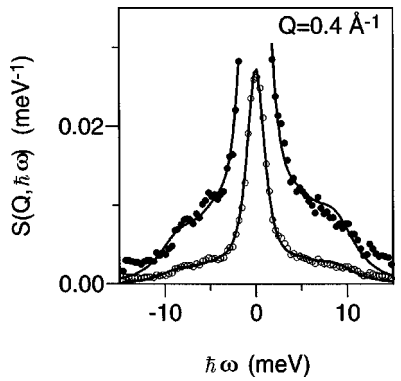

FIG. 9. Dynamic structure factor of light water versus energy transfer at $Q=0.4\,\text{Å}^{-1}$ as obtained by the x-ray scattering measurements of Ref. [3]. The experimental data (circles) are also shown on a scale expanded by a factor of 5 (dots). The solid line is the fit to the x-ray data as obtained by applying the present model described in the text.

$$F^2_{\pm}(Q) \sim Z_{\pm}(Q)\frac{\omega^2_{\pm}}{Q^2}. \tag{9}$$

For $Q \geqslant 0.4\,\text{Å}^{-1}$, $F^2_+(Q)$ is practically constant. Such a behavior would be expected for an unperturbed longitudinal acoustic (LA) mode [15]. The slight decrease of $F^2_+(Q)$ for smaller Q's could be attributed to the fact that, due to the coupling to the opticlike mode ω_0, the structure factor $F^2_+(Q)$ takes up part of the eigenvector of the mode ω_0. The eigenvector of the mode ω_0 is expected to provide a smaller structure factor than the LA mode. $F^2_-(Q)$ at large Q's is mainly attributed to the mode ω_0. The trend of $F^2_-(Q)$ towards smaller Q's is opposite to $F^2_+(Q)$. $F^2_-(Q)$ is increasing because it takes up part of the eigenvector of the LA mode. Within the error bars, $F^2_+(Q)$ and $F^2_-(Q)$ have comparable values at $Q=0.35\,\text{Å}^{-1}$. Therefore we can conclude that the uncoupled modes cross near this value. This means that for larger Q values, $F^2_+(Q)$ is mainly related to the LA mode and $F^2_-(Q)$ to the opticlike mode. The sum $F^2_+(Q)+F^2_-(Q)$ is supposed to be equal to the sum of the individual structure factors $F^2_{\text{LA}}(Q)+F^2_{\omega_0}(Q)$. This quantity is also given in Fig. 10. As we assume that $F^2_{\text{LA}}(Q)$ is independent of Q and $F^2_{\omega_0}(Q)$ should vanish for Q towards zero, we would have expected that the sum decreases for the smaller Q values. However, within the errors the sum remains constant for the Q values investigated here. The other observed Q dependencies of $F^2_{\pm}(Q)$ are in good agreement with our two-mode model.

TABLE I. Experimental values of $Z_{\pm}(Q)$ as deduced from the present data (see text).

Q (Å^{-1})	$Z_-(Q)$	$Z_+(Q)$
0.30	0.0296±0.0014	0.0120±0.0014
0.35	0.0343±0.0014	0.0158±0.0013
0.40	0.0325±0.0012	0.0221±0.0011
0.50	0.0403±0.0009	0.0233±0.0009
0.60	0.0423±0.0010	0.0266±0.0009

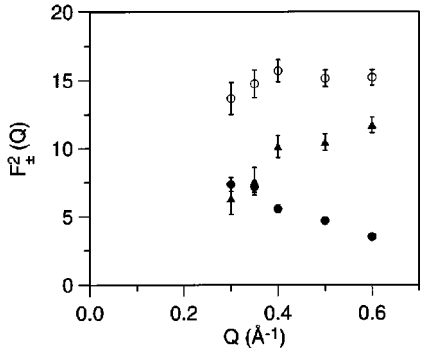

FIG. 10. $F^2_{\pm}(Q)$ provided by the present model versus wavevector transfer (see text). $F^2_-(Q)$, dots; $F^2_+(Q)$, triangles. The sum $F^2_-(Q)+F^2_+(Q)$ is also shown by open circles.

IV. CONCLUSIONS

The present experiment has definitely shown the existence of a complex collective excitation in water when the wavevector transfer is smaller than 0.6 Å^{-1}. This conclusion can be drawn directly from the inspection of the experimental data of Fig. 7. However, more detailed information is obtained from the dispersion relation provided by the model applied to fit the data. The presence of a localized mode with an energy of ~5.5 meV (44 cm^{-1}), which is possibly due to a relative motion of nearest neighbor water molecules, has been clearly identified and found to be in agreement with the results of previous x-ray scattering investigations [3]. Such a mode, with a similar frequency, has been observed in ice [5]. This localized mode has the effect, through the interaction with the unperturbed acoustic mode, of reducing the velocity of the low frequency (perturbed) sound. The present model has the merit of describing the transition from the long wavelength (perturbed) sound to the unperturbed sound in a very simple way, taking into account the now well assessed presence of the localized mode. The unperturbed sound velocity in the liquid, observed as 3200 ± 320 m/s, is much closer to the sound velocity in the solid with about 4000 m/s. An alternative model which can describe the transition from normal to fast sound is employed in Refs. [21], [22] although the presence of the almost dispersionless mode is not taken into account.

The integrated intensities $Z_{\pm}(Q)$, see Eq. (8), as obtained from the fit to the experimental data have also been analyzed. Very generally one can remark that integrated intensities extracted from inelastic neutron scattering data are less reliable than, say, peak positions. Nevertheless, the interpretation of the $Z_{\pm}(Q)$, by plotting the mode structure factors $F^2_{\pm}(Q)$ in Fig. 10, confirms the validity of our model. The model assumes a Q-independent structure factor for the uncoupled LA mode and for the opticlike mode a structure factor which vanishes for Q towards zero.

Finally, the mode strengths obtained by the neutron scattering can be compared with those obtained by fitting the present model to the x-ray data at $Q=0.4\,\text{Å}^{-1}$ as reported in Ref. [3]. From the neutron data at $Q=0.4\,\text{Å}^{-1}$ one has $Z_-=0.0325(12)$ and $Z_+=0.0221(11)$. From the x-ray data, the corresponding values are: $Z_-=0.0109(10)$ and $Z_+=0.0158(10)$. These data show that the visibility of the opticlike mode is smaller in the x-ray dynamic structure factor.

This means that the eigenvector of this mode has larger components on the deuterium atoms.

We are convinced that the description of the low Q collective dynamics of liquid water by means of the present model is quite accurate as it accounts for the observed features of the dynamic structure factor as determined by both neutron and x-ray experiments. Of course, the dynamics of water is far too complex to be fully described by the present small set of parameters. The adequacy of this model in describing the dynamic structure factor suggests, however, that the high number of eigenvectors intervening into the water dynamics contribute mainly to two frequency regions. This picture is in agreement also with the results of the investigation carried out in Ref. [23].

[1] F. Sette, G. Ruocco, M. Krisch, U. Bergmann, C. Masciovecchio, V. Mazzacurati, G. Signorelli, and R. Verbeni, Phys. Rev. Lett. **75**, 850 (1995).

[2] G. Ruocco, F. Sette, U. Bergmann, M. Krisch, C. Masciovecchio, V. Mazzacurati, G. Signorelli, and R. Verbeni, Nature (London) **379**, 521 (1996).

[3] F. Sette, G. Ruocco, M. Krisch, C. Masciovecchio, R. Verbeni, and U. Bergmann, Phys. Rev. Lett. **77**, 83 (1996).

[4] J. Teixeira, M. C. Bellissent-Funel, S. H. Chen, and B. Dorner, Phys. Rev. Lett. **54**, 2681 (1985).

[5] B. Renker, in *Physics and Chemistry of Ice*, paper presented at the Symposium on the Physics and Chemistry of Ice, Ottawa, Canada, August, 1972, edited by E. Whalley, S. J. Jones, and L. W. Gold (Royal Society of Canada, Ottawa, Canada, 1972), pp. 82–86.

[6] F. J. Bermejo, M. Alvarez, S. M. Bennington, and R. Vallauri, Phys. Rev. E **51**, 2250 (1995).

[7] A. Rahman and F. H. Stillinger, Phys. Rev. A **10**, 368 (1974).

[8] M. A. Ricci, D. Rocca, G. Ruocco, and R. Vallauri, Phys. Rev. Lett. **61**, 1958 (1988).

[9] U. Balucani, G. Ruocco, A. Torcini, and R. Vallauri, Phys. Rev. E **47**, 1677 (1993).

[10] F. Sciortino and S. Sastry, J. Chem. Phys. **100**, 3881 (1994).

[11] M. Sampoli, G. Ruocco, and F. Sette, Phys. Rev. Lett. **79**, 1678 (1997).

[12] D. I. Garber and R. R. Kinsey, *Neutron Cross Sections* 3rd ed. (Brookhaven National Laboratory, Upton, NY, 1976), Vol. II, BNL 325.

[13] O. K. Harling, J. Chem. Phys. **50**, 5279 (1969).

[14] *Water. A Comprehensive Treatise*, edited by F. Franks (Plenum, New York, 1972), Vol. 1.

[15] J.-B. Suck, Int. J. Mod. Phys. B **7**, 3003 (1993).

[16] C. Petrillo and F. Sacchetti, Acta Crystallogr., Sect. A: Found. Crystallogr. **46**, 440 (1990).

[17] M. J. Cooper and R. Nathans, Acta Crystallogr. **23**, 357 (1967); B. Dorner, Acta Crystallogr., Sect. A: Cryst. Phys., Diffr., Theor. Gen. Crystallogr. **28**, 319 (1972).

[18] M.-C. Bellissent-Funel, S. H. Chen, and J.-M. Zanotti, Phys. Rev. E **51**, 4558 (1995).

[19] E. Enciso, N. G. Almarza, M. A. Gonzalez, F. J. Bermejo, R. Fernandez-Perea, and F. Bresme, Phys. Rev. Lett. **81**, 4432 (1998).

[20] B. Fak and B. Dorner, Physica B **234-236**, 1107 (1997).

[21] A. Cunsolo, G. Ruocco, F. Sette, C. Masciovecchio, A. Mermet, G. Monaco, M. Sampoli, and R. Verbeni, Phys. Rev. Lett. **82**, 775 (1999).

[22] G. Monaco, A. Cunsolo, G. Ruocco, and F. Sette, Phys. Rev. E **60**, 5505 (1999).

[23] A. Criado, F. J. Bermejo, M. Garcia-Hernandez, and J. L. Martinez, Phys. Rev. E **47**, 3516 (1993).